

## Modeling the Influence of Salt on the Hydrophobic Effect and Protein Fold Stability

Mihir S. Date and Brian N. Dominy\*

*Department of Chemistry, Clemson University, Clemson SC 29631, USA.*

Received 29 July 2011; Accepted (in revised version) 12 October 2011

Available online 12 June 2012

---

**Abstract.** Salt influences protein stability through electrostatic mechanisms as well as through nonpolar Hofmeister effects. In the present work, a continuum solvation based model is developed to explore the impact of salt on protein stability. This model relies on a traditional Poisson-Boltzmann (PB) term to describe the polar or electrostatic effects of salt, and a surface area dependent term containing a salt concentration dependent microscopic surface tension function to capture the non-polar Hofmeister effects. The model is first validated against a series of cold-shock protein variants whose salt-dependent protein fold stability profiles have been previously determined experimentally. The approach is then applied to HIV-1 protease in order to explain an experimentally observed enhancement in stability and activity at high (1M) NaCl concentration. The inclusion of the salt-dependent non-polar term brings the model into quantitative agreement with experiment, and provides the basis for further studies into the impact of ionic strength on protein structure, function, and evolution.

**PACS:** 87.15.K-, 87.15.-v

**Key words:** Electrostatic stability, hydrophobic effect, halophile, cold shock protein, HIV-1 protease.

---

### 1 Introduction

It has long been understood that salts have a significant impact on the stability and activity of proteins and nucleic acids, which constitute a foundation underlying cellular function. The intracellular and extra cellular salt concentration varies with the organism and environment, but fluctuates typically in the range of 100-200 mmol/L for organisms living within physiological conditions consistent with mesophiles. Salts can significantly influence the stability of biomolecules by screening electrostatic interactions. For example, the repulsion between negative charges on the phosphate backbone of nucleic acids

---

\*Corresponding author. *Email addresses:* [mdate@clemson.edu](mailto:mdate@clemson.edu) (M. S. Date), [dominy@clemson.edu](mailto:dominy@clemson.edu) (B. N. Dominy)

is screened by salt, contributing to the stability of biologically relevant DNA and RNA conformations [1]. The effect of salts on proteins has been demonstrated using numerous systems including multimeric complexes that have been shown to disintegrate into separate monomers upon changes in the environmental salt concentration. Some proteins within halophilic organisms have even adapted to function specifically within high salinity environments, destabilizing under physiological salt concentrations consistent with mesophilic environments [2, 3]. The development of accurate physical models describing the thermodynamic impact of salts on macromolecules could lead to a broader understanding of biomolecular structure and function.

Within a cellular environment, biomolecules are solvated in an aqueous environment containing salt ions and numerous other solutes. The influence of ions on biomolecular interactions is mediated through electrostatic screening, site-specific binding, and preferential hydrophobic effects or Hofmeister effects. The role of salt concentration in protein stability can be determined by measuring the unfolding transition as a function of salt concentration, but interpreting the mechanism of action is a non-trivial problem. Some ions stabilize proteins by binding to specific sites. This ligand-induced ion-specific stabilization is usually observed below 0.2 mol/L ionic strength [4]. Bulk ionic strength results in the screening of surface charge-charge interactions primarily at lower salt concentrations. Hofmeister effects, which are dominant at higher salt concentrations, strengthen the hydrophobic effect by increasing the surface tension of the solvent, or by stabilizing peptide dipoles through specific ionic interactions [5]. Theoretical modeling can provide a basis from which the different mechanisms associated with salt effects may be assessed and compared.

The electrostatic screening effect (and the effect on self polarization energies), primarily related to bulk ionic strength, can be studied through continuum electrostatic models such as those based on a Poisson-Boltzmann (PB) formalism [6,7]. The PB equation can be used to describe the electrostatic potential from the reaction field of a system containing a solute with a fixed charge distribution and a surrounding mobile charge distribution representing the salt. Mobile charges are modeled by a Boltzmann distribution with respect to the electrostatic potential generated by the fixed charges of the solute [8]

$$\begin{aligned} & \vec{\nabla} \cdot [\epsilon(\vec{r}) \vec{\nabla} \phi(\vec{r})] \\ &= -4\pi p^f(\vec{r}) - 4\pi \sum_i c_i^\infty Z_i \lambda(\vec{r}) \cdot e^{-Z_i \phi(\vec{r}) / \kappa_\beta T}. \end{aligned} \quad (1.1)$$

Eq. (1.1) is the Poisson-Boltzmann equation, which describes electrostatic interactions between solute and solvent molecules where  $p^f$  is charge density of fixed charges.  $c_i^\infty$  is the concentration of ion  $i$  and  $Z_i$  is the charge of the ion. The second term on right hand side represents mobile charges typically restricted to the solvent region. It contains the ionic strength and charge density associated with the mobile charges. The distribution of mobile charges around solute's fixed charges is modeled by the Boltzmann factor ( $e^{-Z_i q \phi(\vec{r}) / \kappa_\beta T}$ ). This special case of Debye-Hückel theory with a 1:1 electrolyte accounts

for continuum solvent polarization effects involving a salt distribution around the solute [9]. Using this model, the electrostatic free energy of solvation can be determined, as well as the role of ionic strength on electrostatic screening.

While PB (or generalized Born [10]) models are used to calculate polar component of the solvation free energy and the role of ionic strength, surface area based models are popular in accounting for the non-polar hydrophobic component. These models express the non-polar solvation term as linearly proportional to the solute's surface area. The most famous being the cavity model developed by Sitkoff et al., which is based on partition coefficients for a series of hydrocarbons [11]

$$\Delta G_{non-polar} = \gamma \times ASA. \quad (1.2)$$

The cavity model based on scaled practical theory expresses the non-polar solvation energy as a product of the solute's solvent accessible surface area (*ASA*) and a proportionality constant described as the microscopic solute-solvent surface tension ( $\gamma$ ) [12]. Recently, alternative models describing the hydrophobic effect have been described in the literature. Some alternative models involve the inclusion of dispersion integrals and solvent accessible volume terms [13,14]. They indicate that the work of cavitation for a solute should depend on its solvent accessible surface area (*SASA*) and solvent accessible volume (*SAV*), with the *SASA* term dominating for large solutes. Another popular model to account for non-polar solute-solvent interactions is the dewetting model [15]. This model accounts for non-polar forces acting on a surface through the critical distance between surfaces in contact, the contact angle and surface tension of water.

While both of these models provide alternatives to the cavity model to estimate the non-polar component of solvation free energy, the cavity model has been validated numerous times in the literature. In addition, its simplicity and current wide-spread use suggested this model for the current study. Parameterized for aqueous solutions, the cavity model provides a quantitative description of the hydrophobic effect at a molecular scale. The model is based on the macroscopic description of surface free energy or surface tension. The solute solvent microscopic interface on the surface of biological macromolecules is far different than an oil-water or water-air macroscopic interface. The cavity model therefore requires the predetermination of a microscopic surface tension parameter that should also be dependent on the environmental salt concentration.

Here we develop a model to describe the effect of ionic strength on protein fold stability involving traditional PB continuum electrostatic theory and a surface area based hydrophobic term. The cavity model used here includes a microscopic surface tension that is now described as a function of ionic strength. We validate our model by calculating the effect of ionic strength on the stability of a family of Cold Shock Proteins (*CSP's*). Further we successfully apply our model toward the HIV-1 protease enzyme (*HIV-PR*) to discover the mechanisms underlying the experimentally observed influence of NaCl on stability and activity. The results from these calculations are found to be in close agreement with corresponding experimental results [16,17].

## 2 Methods and materials

### 2.1 Protein and enzyme models

We have studied the effect of salt on the fold stability of the cold shock protein family derived from the mesophilic bacterium *Bacillus subtilis* (Bs-CspB) and the thermophilic bacterium *Bacillus caldolyticus* (Bc-Csp). We used the wild type and mutants from these proteins to authenticate our model describing the effect of salt through both electrostatic and hydrophobic contributions to the free energy. The crystal structures of the cold shock proteins, 1CSP and 1C9O, were used as a starting point [18, 19]. A gentle minimization technique, involving a stepwise reduction in a harmonic force constraint, was applied to the CSP crystal structures using the CHARMM (c32b1) molecular mechanics package [20]. All minimized structures yielded an RMSD below 0.7 Å relative to the corresponding crystal structures. Mutants of these proteins were modeled using MODELLER software package [21]. The mutants modeled and examined in this study are E3R, E3L, A46E, E66L, E3R/E66L, E3R/T64V/E66L for Bs-CspB and L66E, Q53E, E46A, T31S, S24D, G23Q, E21A, Y15F, N11S, R3E, R3L, R3A, Q2L, R3E/E46A/L66E, G23Q/S24D, R3E/L66E, R3E/E21A, R3E/E46A, E46A/L66E for Bc-Csp. Mutated residues were minimized in the context of a fixed protein environment in order to remove vdW clashes and improve electrostatic interactions.

The presently available structures of unbound HIV-PR include different types of conformations including semi-open, open and curled. Wild type structures of the semi-open and curled conformation are available. To investigate the increased stability with increased salt concentration of HIV-PR, two crystal structures of HIV-PR viz 1HHP (semi-open) and 3PHV (curled) from the protein databank were used [22, 23]. HIV-PR has two aspartate residues, ASP 25 and ASP 25', in its active site that are essential to its catalytic activity. Numerous theoretical and experimental studies have been performed in the past to determine protonation state of these aspartates in the active site of HIV-PR dimer [24, 25]. Work by Smith et al. on HIV-PR, through C<sup>13</sup> NMR experiments, suggests that HIV-PR in its unbound state shows two chemically equivalent aspartic side chains in the catalytic site and they are ionic [26]. Hence, we modeled the catalytic aspartates in their ionic state. Coordinates of the structures were taken from RCSB Protein Data Bank. Any missing atoms in the crystal structures were added and then minimized using the same strategy applied to the CSP wild type structures within the CHARMM (c32b1) molecular mechanics package.

### 2.2 Calculating the "Salt effect": The polar or electrostatic component

As described earlier, the solvation free energy is composed of two components: the electrostatic or polar and the hydrophobic or non-polar components

$$\Delta G_{\text{solvation}} = \Delta G_{\text{elec}} + \Delta G_{\text{non-polar}}. \quad (2.1)$$

Using the PB model, the electrostatic component of the unfolding free energy ( $\Delta G_{el}(I)$ ) can be calculated as a difference between the unfolded and folded states of a protein

$$\Delta G_{el}(I) = G_{el}^u(I) - G_{el}^f(I), \quad (2.2)$$

where  $G_{el}^u(I)$  is the electrostatic free energy of unfolded state and  $G_{el}^f(I)$  is the electrostatic free energy of folded state at some ionic strength ( $I$ ). The unfolded state is the point where tertiary and most secondary structure is lost, and is modeled here by assuming each residue ( $i$ ) interacts only with its two sequential neighbors on each side ( $i-2, i-1, i+1, i+2$ ). The local conformation of this five residue segment representing the unfolded state is kept unaltered as it appears in the folded state. A properly normalized sum, over all the residues, of the self and interaction (Coulombic and cross-polarization) energies of each residue in the middle of the segment, preventing the double counting of interaction energies, is the total electrostatic free energy of unfolded state. Thus, the electrostatic free energy of the unfolded state becomes

$$G_{el}^u(I) = \sum_1^N G_{el}(I), \quad (2.3)$$

where  $N$  is total number of residues in the protein. The same unfolded state model was used in an earlier study where it was also compared to alternative models of the unfolded state [27]. In this study, the electrostatic component of salt effect was shown to be robust towards the choice of unfolded state model. Structure-based thermodynamic analyses of HIV-PR indicate the folding of individual monomers occurs prior to the dimerization of monomers, resulting in the final and active conformer [28, 29]. Consequently, in the case of HIV-PR, in addition to the unfolding free energy of monomers shown by Eq. (2.3), the contribution from the dissociation of the dimer was also included to account for total free energy of unfolding. It can be shown as

$$G_{el}^{F-D}(I) = G_{el}^A(I) + G_{el}^B(I), \quad (2.4)$$

where  $G_{el}^A(I)$  and  $G_{el}^B(I)$  are the electrostatic free energies of folded monomer  $A$  and monomer  $B$  and  $G_{el}^{F-D}(I)$  is energy of folded dimer of HIV-PR. The two contributions from dimer dissociation and monomer unfolding were simply added together to account for total unfolding free energy of HIV-PR. The salt dependence of the unfolding free energy, or the "salt effect"  $\Delta\Delta G_{el}(I)$ , is the difference in the electrostatic component of unfolding free energy calculated at some ionic strength and reference ionic strength ( $I'$ )

$$\Delta\Delta G_{el}(I) = \Delta G_{el}(I) - \Delta G_{el}(I'). \quad (2.5)$$

The model used to calculate the electrostatic free energy of unfolding involved a finite difference solution of the linearized Poisson-Boltzmann equation and a thermodynamic cycle that involved a structural model for folded and unfolded states [30]. Charged states

of titratable residues for folded as well as unfolded state models of all CSP and HIV-PR structures were assigned based on their isolated states at neutral pH. It is neither intended nor within the scope of this study to explicitly incorporate the effect of pH while investigating the salt effect on protein fold stability. In order to see the effect of surrounding pH along with salt effect studies, an appropriate methodology can be utilized to first calculate the pKa's and corresponding charged states of titratable residues in both the folded and unfolded conformations at each solution ionic strength. Poisson-Boltzmann calculations [8] were performed within the CHARMM (c32b1) molecular mechanics package. The grid parameters chosen included a grid point density of  $0.5 \text{ \AA}^{-1}$ , and a grid size of  $50 \text{ \AA}^3$  and  $68 \text{ \AA}^3$  for CSP and HIV-PR respectively. A variety of different grid spacings were examined and the polar salt effect was found to converge at a grid density of  $0.5 \text{ \AA}^{-1}$ . Atomic charges and vdW radii were assigned according to CHARMM param27 all hydrogen force field. The vdW molecular surface was chosen for electrostatic as well as hydrophobic term calculation.

The hydrophobic solvation term was simply added to the component related to the electrostatic solvation free energy to provide a model of the salting out contribution to protein stability with increasing salt effect. The protein dielectric constant is not a universal constant but a parameter that depends on the model used [31]. Theoretical studies on different proteins and enzymes have been performed with protein interior dielectric constants varying from 2 to 20. [6, 32–35]. Salt effect studies were conducted on CSP as well as HIV-PR using protein interior dielectrics of 2, 4 10 and 20 (data not shown). While all of them recapitulated the same qualitative results, a dielectric of 4 resulted in the best quantitative agreement with experimental data. Consequently, a protein interior dielectric constant of 4 was used in modeling both CSP and HIV-PR. This value for the interior protein dielectric constant has also been used previously and was shown to yield accurate results [27, 35]. The dielectric constant for the surrounding continuum solvent water was assigned a value of 80.

### 3 Results and discussion

#### 3.1 The non-polar solvation energy as a function of ionic strength

We calculated the change in stability of CSP with increasing salt concentration known as the salt effect. An increasing salt concentration influences protein stability in mainly two ways. The first is through electrostatic influences on self-polarization energy and cross-polarization energy, or screening of electrostatic interactions. This effect is predominant for all types of salt typically below a concentration of 0.5 mol/L. The second is through the surface tension defined at the solute-solvent interface, which increases with an increase in the salt concentration. In an aqueous solvent, this increase in the surface tension increases the hydrophobic effect [36–38] (Eq. (1.2)). Consequently to calculate the true salt effect on protein stability, it is important to take into account the hydrophobic effect along with the electrostatic contribution to the unfolding free energy [11]. Our

model uses a cavity model to describe the non-polar or hydrophobic component of solvation (Eq. (1.1)).

The relationship between the microscopic surface tension and the well-known macroscopic analog provides the basis for a more generalized theory of non-polar solvation and the corresponding hydrophobic effect. The free energy associated with the transfer of a non-polar solute from oil into water (microscopic) and the interfacial free energies between non-polar liquids and water (macroscopic) provide alternate measures of the free energy per unit area or the 'surface tension'. Based on published data, these two measures of surface free energy are mutually inconsistent [39]. While macroscopic surface tension can be measured directly through experiments, microscopic surface tension is estimated through the transfer free energy of solutes. Shown through solvent transfer experiments for wide range of hydrocarbon molecules, hydration free energy depends linearly on the burial of solvent accessible surface area. Based on experimentally determined transfer free energies, a microscopic surface tension value ( $\gamma_{micro}$ ) was determined. It ranges from 25 cal/ $\text{\AA}^2$  to 31 cal/ $\text{\AA}^2$  for different groups of alkanes including linear ( $28 \pm 2$  cal/mol $\cdot\text{\AA}^2$ ), branched (31 cal/mol $\cdot\text{\AA}^2$ ) as well as cyclic and aromatic (25 cal/mol $\cdot\text{\AA}^2$ ) [12,40,41]. These groups best mimic amino acid side chains in proteins and enzymes and thus the microscopic surface tension parameter derived from hydration free energies through solvent transfer experiments of these groups can be used towards the evaluation of the non-polar or hydrophobic component of the solvation free energy of proteins. We take the average microscopic surface tension from the different classes of hydrocarbon solutes that best mimic side chains from amino acids residues. The average value for ( $\gamma_{micro}$ ) comes to 28 cal/ $\text{\AA}^2$ , which is almost two-fifths of the macroscopic oil-water interface surface tension value ( $\gamma_{macro}$ ) of 72 cal/ $\text{\AA}^2$  [40,42,43]. Selection of this value is consistent with the type of surface area used in PB electrostatic calculations.

To develop a model of the microscopic surface tension as a function of ionic strength, we begin with the macroscopic oil-water interface surface tension of approximately 72 cal/ $\text{\AA}^2$  or 0.3 kJ/ $\text{\AA}^2$ . The surface tension of electrolyte solution increases with increase in ionic strength. Under isobaric and isothermal conditions, the dependence of the surface tension on the electrolyte concentration can be given from Gibbs adsorption equation [44]

$$d\gamma = -\sum_i \Gamma_i d\mu_i, \quad (3.1)$$

where  $\Gamma_i$  is surface excess/deficiency of ion  $I$ , and  $\mu_i$  is the chemical potential of the salt ions at the interface. In this relation both of the parameters  $\mu_i$  and  $\Gamma_i$  are dependent of the concentration of salt ions in the solution. Eq. (3.1) describes the dependence between the surface tension of an electrolyte solution and its ionic strength. In order to calculate the non-polar component of the solvation free energy as a function of ionic strength, it is essential to accurately calculate the increment in surface tension rather its absolute value.

The increment in macroscopic surface tension as a function of NaCl concentration ( $\partial\gamma_{macro}/\partial I$ ) is 1.64 dynes/cm $^2$ /M or 9.9 J/ $\text{\AA}^2$ molM [44,45], where M refers to the molar concentration of NaCl. This value varies with the specific salt used, but is similar for 1:1

salts such as NaCl or KCl. This derivative of the macroscopic surface tension remains constant up to a salt concentration of 1 mol/L. Similarly, the salt concentration should have a corresponding impact on the microscopic surface tension. We assume that the impact of the salt concentration on the microscopic surface tension will be reduced but still enables the ions to raise the surface energy at the interface and will be smaller by the same proportion between macro and microscopic surface tension. Based on the fact that the microscopic surface tension value ( $\gamma_{micro}$ ) chosen in this study, is approximately 2/5 of the macroscopic surface tension value ( $\gamma_{macro}$ ), we assume that the increment in microscopic surface tension with increasing ionic strength ( $\partial\gamma_{micro}/\partial I$ ) is 2/5 of the value associated with the macroscopic surface tension ( $\partial\gamma_{macro}/\partial I$ ). Thus, the partial derivative ( $\partial\gamma_{micro}/\partial I$ ) becomes

$$\frac{\partial\gamma_{micro}}{\partial I} = \frac{1}{2.6} \cdot \frac{\partial\gamma_{macro}}{\partial I}. \quad (3.2)$$

Eq. (3.2) enables us to calculate increase in microscopic surface tension with ionic strength. As the macroscopic surface tension increases linearly with increasing ionic strength, we assume increment in microscopic surface tension will stay constant up to a salt concentration of 1 mol/L. Based on the facts and assumptions stated above, the salt concentration dependent microscopic surface tension becomes

$$\gamma_{micro}(I) = \gamma_{micro}(0) + \frac{\partial\gamma_{micro}}{\partial I} \cdot I. \quad (3.3)$$

Using Eqs. (3.2) and (3.3), it is possible to calculate the microscopic surface tension as a function of ionic strength. This can be straightforwardly used in conjunction with the cavity model to estimate the non-polar or hydrophobic component of the solvation free energy as a function of ionic strength.

### 3.2 Assessing the model: Fold stability of CSP variants as a function of ionic strength

After describing how salt influences electrostatic screening and the hydrophobic effect, we validated our model by calculating the salt effect on fold stability of the cold-shock protein (CSP) family and several associated mutants. CSP's are small, monomeric proteins expressed by mesophilic *Bacillus subtilis* (Bs-CspB) and thermophilic *Bacillus caldolyticus* (Bc-Csp). Within the CSP family, the mesophilic protein was reported to show an increasing stability while decreasing stability was reported for the thermophilic protein with increasing NaCl concentration [19]. It was found that the increased stability of Bs-CspB originates entirely from two residues, which are E3 and E66 in Bs-CspB while in the thermophile these positions correspond to R3 and L66 [46]. Salt screens the unfavorable pair wise Coulombic interaction between E3 and E66 in Bs-CspB, resulting in a halophilic response with increasing ionic strength. Experimentally, the unfolding free energies of 19 variants of Bc-Csp and 6 variants of Bs-CspB have been determined under a variety of ionic strength conditions [17]. The effect of ionic strength was studied

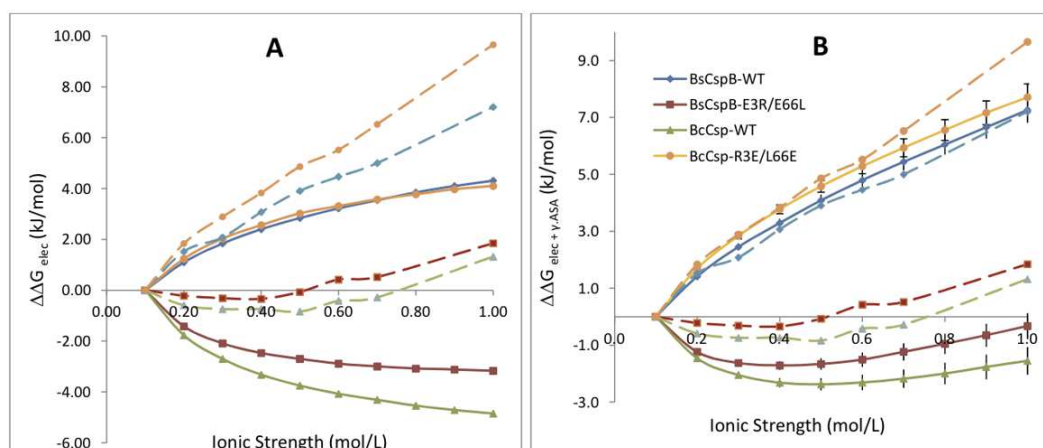


Figure 1: Salt effect on stability of CSP. A. Calculated electrostatic contribution to protein stability using our theoretical model (solid lines) B. Calculated stability including electrostatic contribution and hydrophobic term using our model. Experimental unfolding free energy as a function of NaCl concentration are shown by dashed lines in A as well as B. Only when the hydrophobic term is added to the electrostatic component of solvation free energy do the theoretical calculations agree with experimental results. The experiments were conducted in a buffer of 0.1mol/L ionic strength. To match this, our reference point for calculating the salt effect is 0.1mol/L and not zero. The error bars in B show the limits of the model based on the previously described range of microscopic surface tension parameters (between 25 and 31 cal/Å<sup>2</sup>mol).

previously but was restricted only to the electrostatic component of the free energy of solvation [27,35].

The influence of ionic strength on the stability of the cold shock protein family is shown in Fig. 1. The solid lines in Fig. 1A show the salt effect involving only the electrostatic component determined through our calculations, while the solid lines in Fig. 1B show the more complete salt effect involving both electrostatic and hydrophobic components calculated through our model. Dashed lines Figs. 1A and B both, represent the experimentally determined salt effect [17]. These figures clearly demonstrate that the electrostatic influence of ionic strength toward fold stability is insufficient to reproduce the experimentally observed behavior. The electrostatic stability profile shows good qualitative agreement but is insufficient in providing quantitative agreement with experiment. The saturating effect of the electrostatic stability in Fig. 1A was seen as the ionic strength was increased above  $\sim 0.5$  mol/L. This is not seen in the experimental results as these represent a combination of electrostatic as well as hydrophobic influences on protein stability. At higher salt concentrations, although the electrostatic effect saturates, increases in surface tension and the hydrophobic force continue to stabilize the protein fold. Inclusion of the ionic strength dependent microscopic surface tension through the cavity model accounts for the enhanced fold stability through the hydrophobic effect at higher salt concentrations, while not significantly impacting the predicted changes in fold stability at salt concentrations below 0.5 mol/L. The result is a model with improved agreement with experimental studies over a broader range of ionic strength. This is seen

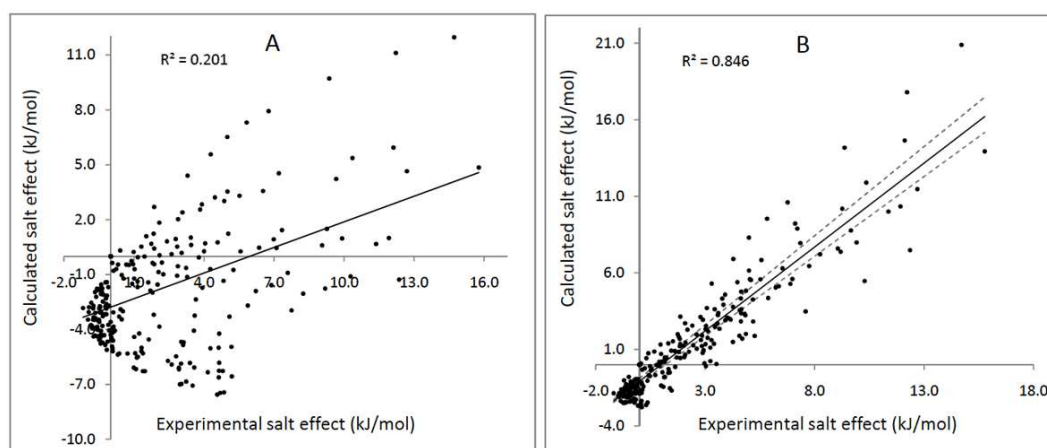


Figure 2: Comparing experimental and calculated salt effect data. A. Calculated values include only electrostatic term. B. Calculated values include the electrostatic and hydrophobic terms. Data points represent 27 structures studied from 0.1 mol/L to 1.0 mol/L ionic strength giving 243 data points in total. The correlation between experimental and calculated results improves drastically from A to B. Dotted lines show upper and lower limits of model using microscopic surface tension at extremes (25 and 31 cal/Å<sup>2</sup>mol).

from Fig. 1B where the theoretical data demonstrate excellent agreement with experimental data. The hydrophobic effect is dominant and the electrostatic screening effect of salt is saturated at high ionic strengths typically from 0.7 mol/L to 1.0 mol/L. Therefore, in the same range of ionic strength, the change in the free energy of solvation as a function of ionic strength is coming almost entirely from the hydrophobic effect. The average change in the free energy, based on the experimental results between 0.7 mol/L to 1.0 mol/L ionic strength, is found to be 4.13 ( $\pm 1.3$ ) kJ/mol. The corresponding average change in free energy based on the model over the same NaCl concentration range is 3.01 ( $\pm 1.1$ ) kJ/mol. The close agreement between the theory and experiment provides further evidence supporting the validity of the microscopic surface tension function developed in this study.

After observing the qualitative and quantitative behavior of the salt effect model applied to four representative CSP structures, we applied the same model to the entire set of CSP structures to assess the validity of our model. Fig. 2 demonstrates the broader agreement between experimental and calculated data over a variety of protein variants and salt conditions. It shows a comparison between salt-dependent protein stabilities determined from experimental data and calculations using over 27 mutant structures from the CSP family at ionic strengths ranging from 0.1 mol/L to 1.0 mol/L. The correlation between the electrostatic component and experimental unfolding free energies (Fig. 2A) is very poor ( $R^2 = 0.21$ ), but increases dramatically ( $R^2 = 0.87$ ) when the hydrophobic or salting out term is added to calculated electrostatic unfolding free energy (Fig. 2B).

Table 1 summarizes data points from Fig. 2 only at 0.1 mol/L and 1.0 mol/L salt concentrations. It clarifies the difference between the experimental data set and two sets of theoretical calculations. It is seen that in comparison to the experimental results, at 0.1

Table 1: The difference between the experimental data and two sets of calculated data using our model.  $\Delta\Delta G_{elec}$  describes only the electrostatic component while  $\Delta\Delta G_{elec} + \gamma \cdot ASA$  describes both the electrostatic and hydrophobic components of solvation free energy.  $\langle \Delta\Delta\Delta G \rangle$  (in kJ/mol), is the average difference between  $\langle \Delta\Delta G \rangle$  for two sets of theoretical calculations. Numbers in bracket represents error estimation using microscopic surface tensions ( $\gamma_{micro}$ ) at extremes (25 and 31 cal/Å<sup>2</sup>mol).  $\langle \Delta\Delta\Delta G \rangle$  is around 10 fold larger going from 0.1 to 1.0 mol/L salt concentration demonstrating the importance of including the hydrophobic effect.

	At 0.1 mol/L salt conc.		At 1.0 mol/L salt conc.	
	$\Delta\Delta G_{elec}$	$\Delta\Delta G_{elec} + \gamma \cdot ASA$	$\Delta\Delta G_{elec}$	$\Delta\Delta G_{elec} + \gamma \cdot ASA$
$\langle \Delta\Delta G \rangle$	-1.07	-0.61(±0.05)	-5.73	-1.14 (±0.4)
$\langle \Delta\Delta\Delta G \rangle$	0.46		4.61	

mol/L theoretical calculations involving only electrostatic component under predict by only 1.07 kJ/mol. Relative to the electrostatic component, the hydrophobic influence is negligible at 0.1 mol/L. After adding the hydrophobic term, the agreement between the theory and experiment improves though slightly. The average difference ( $\langle \Delta\Delta\Delta G \rangle$ ) between two sets of calculations is very small ( $\langle \Delta\Delta\Delta G \rangle = 0.46$  kJ/mol) demonstrating that the magnitude of the hydrophobic effect is minimal at low ionic strengths and salt primarily plays a role of screening electrostatic interactions at low ionic strength. However, at 1.0 mol/L ionic strength, the average error between two sets of calculations is much larger ( $\langle \Delta\Delta\Delta G \rangle = 4.61$  kJ/mol). This demonstrates that at high ionic strength the hydrophobic or non-polar component becomes a significant and even dominant mechanism underlying the effect of salt on protein stability.

Our model demonstrates very good agreement with experimental results; however a perfect match is not expected. Currently, our model neglects specific ionic interactions and Hofmeister effects. These specific ionic interactions are negligible at low salt concentration but their influence increases with increasing salt concentration. In addition, the unfolded reference state chosen in our model is not necessarily representative of the true denatured state ensemble. Our unfolded state model for all CSP variants is same and presumes no long-range interactions. The experimental data reports thermally denatured proteins where protein unfolded state may not be extended random coils. Our unfolded state for CSP likely provides an upper bound on the true influence of salt on protein fold stability.

### 3.3 Fold stability of HIV-PR as a function of ionic strength

Following the validation of our model on the CSP family, we then applied it toward characterizing the ionic strength dependent fold stability of HIV protease. Interestingly, though mesophilic in nature, HIV-PR has been shown to exhibit increased stability and catalytic activity with increasing salt concentration [16]. It was pointed out that  $K_m$  values, integral to effective rate constants in enzymatic catalysis, are dependent on conditions like pH and salt concentrations [47]. These environmental factors can manifest their influence on catalytic rate through enzyme conformational stability. Through this study,

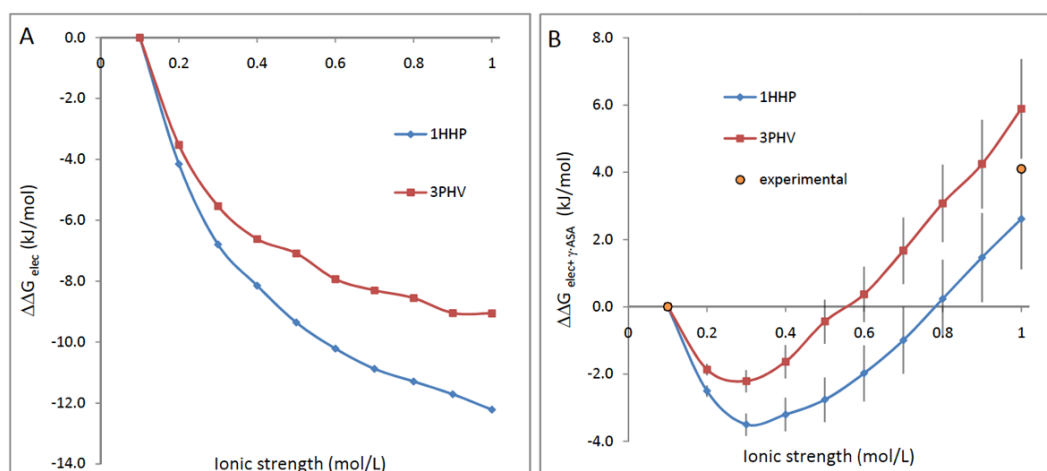


Figure 3: Free energy of unfolding of HIV-PR as a function of ionic strength. A. Electrostatic stability profiles based on two independent unliganded wild type crystal structures of HIV-PR as a function of ionic strength. B. Unfolding free energy accounting for both electrostatic stability and the hydrophobic component. From the electrostatic point of view, both of the structures show decreasing stability with increasing ionic strength with the curled structure (3PHV) being destabilized more than semiopen (1HHP). Error bars in B show the limits of the model using microscopic surface tension parameters at extremes (25 and 31 cal/Å<sup>2</sup>mol).

we seek to determine the physical basis underlying the effect of ionic strength on the conformational stability of HIV-PR, and its relation to the activity of this enzyme.

In order to analyze the stability of HIV-PR, we first calculate the electrostatic contribution of the unfolding free energy with increasing ionic strength. From electrostatic calculations shown in Fig. 3, HIV-PR is destabilized with increasing ionic strength and tends toward a saturation point. Despite the proximal and negatively charged catalytic aspartates in the dimerized folded state, HIV protease does not exhibit halophilic properties at low or physiological ionic strength. Our results are plotted starting from 6 mmol/L ionic strength, calculated based on the buffer solution described in the corresponding experimental study [16].

Our results involving only the electrostatic stability of HIV-PR do not match with experimental values, which demonstrates an enhanced fold stability upon the addition of 1.0M NaCl [16]. It shows that the electrostatic component alone is insufficient in providing a complete description of the influence of salt on the stability of HIV-PR. Upon the inclusion of the salt dependent hydrophobic solvation model, we achieve better agreement with experimental results. The results achieved with the more complete salt-dependent model are shown in Fig. 3B.

Our results after adding the non-polar or hydrophobic component are in close agreement with the experimental data, once again demonstrating the importance of the salt effect through the hydrophobic mechanism. This can be seen directly by comparing results in Figs. 3A and 3B for the salt effect of HIV-PR at 1.0 mol/L salt concentration. For clarity, it should be noted that this does not imply that the hydrophobic effect is primarily

responsible for the stability and functioning of the enzyme, but simply that the influence exerted by NaCl on the stability of HIV protease is primarily described through Hofmeister effects.

Comparing Fig. 1 for CSP and Fig. 3 for HIV-PR, we can observe that difference between polar and non polar components of solvation free energy, in going from 0.1 mol/L to 1.0 mol/L ionic strength, in the case of two HIV-PR structures ( $\sim 14$  kJ/mol) is almost 3.5 times as much than that for CSP family ( $\sim 4$  kJ/mol). This is expected as the surface area of HIV-PRs ( $\sim 4200$  Å<sup>2</sup>,  $\sim 3380$  Å<sup>2</sup> form monomer unfolding and  $\sim 900$  Å<sup>2</sup> upon dimer separation) and CSP family ( $\sim 1200$  Å<sup>2</sup>) share a similar relationship. The surface tension function that mediates the relationship between the change in surface area and the non-polar solvation free energy is applied identically to both the HIV-PR and CSP systems.

### 3.4 The influence of salt on conformational equilibria and activity of HIV-PR

HIV-PR in its unliganded form is known to adopt a variety of functionally important conformations. NMR experiments have established the flexibility of the flap region, suggesting that closed, semi-open, and fully open conformations of the protease are in dynamic equilibrium, with the semi-open form being prevalent for the free protease [48]. Understanding this issue of flap mobility and the associated conformational equilibria has profound implications on the mechanism and activity of the protease. Though the semi-open conformation is more populated, a curled conformation is also observed during the opening event in which the flap tips are curled back toward the protease burying additional hydrophobic sidechains. Flap curling serves as trigger for flap opening and facilitates substrate binding [49,50]. Our calculations indicate that salt effects, arising both from polar and non-polar contributions, preferentially stabilize the curled conformation (3PHV) relative to the semi-open conformation (1HHP). The enhanced activity of HIV protease observed at higher NaCl concentrations could be the result of two effects. First, the enhanced stability of the folded conformation of the protease (a weakly stable enzyme under physiological conditions) at higher NaCl concentrations could lead to enhanced activity simply as the result of an increased population of functional enzyme. Second, the selective stabilization of the functionally important curled conformation could also contribute to the enhanced catalytic activity observed at higher NaCl concentrations.

## 4 Conclusions

Here we have described a theoretical model to qualitatively and quantitatively evaluate the electrostatic effects and hydrophobic effects of salt on protein and enzyme fold stability. One unique aspect of this model is the inclusion of an ionic strength dependent microscopic surface tension used to address the influence of salt on the non-polar solvation energy. Utilizing this salt-dependent model of protein stability, we have demonstrated excellent agreement with experimental results determined for a substantial collection of

27 cold-shock protein variants. The model illustrates a balance whereby the influence of salt at low concentrations is exerted primarily through electrostatic screening, while at higher concentrations the effect is exerted primarily through non-polar solvation (often characterized as hydrophobic effects in aqueous solvents). Both of these physical mechanisms underlying the salt effect must be properly accounted for to properly describe the influence bulk ionic strength.

The model was further applied to the HIV protease system in order to better understand the experimental observation of enhanced stability and activity in high (1M) concentrations of NaCl. The results of the ionic-strength dependent stability calculations, applied to x-ray structures of the unliganded HIV protease, once again demonstrate excellent agreement with experimental measurements. In addition, calculations performed on two catalytically important conformations of the protease, the semi-open and curled conformations, indicate a preferential stabilization of the curled conformation at high NaCl concentrations. Prior work establishing the importance of this conformation in the initiation of catalytic activity suggests this preferential stabilization as a contributor to the enhanced activity observed at these conditions.

## Acknowledgments

This work is supported by the NSF CAREER Award (MCB-0953783). We acknowledge the help of Dr. Dieter Perl and Dr. Franz Schmid for providing the experimental data regarding the salt effect on cold shock proteins.

## References

- [1] C. Schildkraut and S. Lifson, Dependence of the melting temperature of DNA on salt concentration, *Biopolymers*, 3 (1965), 195-208.
- [2] G. Zaccai and H. Eisenberg, Halophilic proteins and the influence of solvent on protein stabilization, *Trends in Biochemical Sciences*, 15 (1990), 333-337.
- [3] J. K. M. Rao and P. Argos, Structural stability of halophilic proteins, *Biochemistry*, 20 (1981), 6536-6543.
- [4] E. R. Goedken and S. Marqusee, Co-crystal of escherichia coli mase hi with mn<sup>2+</sup> ions reveals two divalent metals bound in the active site, *Journal of Biological Chemistry*, 276 (2001), 7266-7271.
- [5] M. T. Record Jr, W. Zhang and C. F. Anderson, Analysis of effects of salts and uncharged solutes on protein and nucleic acid equilibria and processes: A practical guide to recognizing and interpreting polyelectrolyte effects, hofmeister effects, and osmotic effects of salts, in: D. S. E. Frederic, M. Richards and S. K. Peter (Eds.) *Advances in Protein Chemistry*, Academic Press, 1998, pp. 281-353.
- [6] A. H. Elcock and J. A. McCammon, Electrostatic contributions to the stability of halophilic proteins, *Journal of Molecular Biology*, 280 (1998), 731-748.
- [7] R. L. Baldwin, How hofmeister ion interactions affect protein stability, *Biophysical Journal*, 71 (1996), 2056-2063.

- [8] W. Im, D. Beglov and B. Roux, Continuum solvation model: Computation of electrostatic forces from numerical solutions to the poisson-boltzmann equation, *Computer Physics Communications*, 111 (1998), 59-75.
- [9] A. Nicholls and B. Honig, A rapid finite difference algorithm, utilizing successive over-relaxation to solve the poisson-boltzmann equation, *Journal of Computational Chemistry*, 12 (1991), 435-445.
- [10] D. Bashford and D. A. Case, Generalized born models of macromolecular solvation effects, *Annual Review of Physical Chemistry*, 51 (2000), 129-152.
- [11] D. Sitkoff, K. A. Sharp and B. Honig, Accurate calculation of hydration free energies using macroscopic solvent models, *The Journal of Physical Chemistry*, 98 (1994), 1978-1988.
- [12] D. Sitkoff, K. A. Sharp and B. Honig, Correlating solvation free energies and surface tensions of hydrocarbon solutes, *Biophysical Chemistry*, 51 (1994), 397-409.
- [13] J. A. Wagoner and N. A. Baker, Assessing implicit models for nonpolar mean solvation forces: The importance of dispersion and volume terms, *Proceedings of the National Academy of Sciences*, 103 (2006), 8331-8336.
- [14] E. Gallicchio, M. M. Kubo and R. M. Levy, Enthalpy-entropy and cavity decomposition of alkane hydration free energies: Numerical results and implications for theories of hydrophobic solvation, *The Journal of Physical Chemistry B*, 104 (2000), 6271-6285.
- [15] X. Huang, C. J. Margulis and B. J. Berne, Dewetting-induced collapse of hydrophobic particles, *Proceedings of the National Academy of Sciences of the United States of America*, 100 (2003), 11953-11958.
- [16] Z. Szeltner and L. Polgár, Conformational stability and catalytic activity of hiv-1 protease are both enhanced at high salt concentration, *Journal of Biological Chemistry*, 271 (1996), 5458-5463.
- [17] D. Perl and F. X. Schmid, Electrostatic stabilization of a thermophilic cold shock protein, *Journal of Molecular Biology*, 313 (2001), 343-357.
- [18] H. Schindelin, M. A. Marahiel and U. Heinemann, Universal nucleic acid-binding domain revealed by crystal structure of the b. Subtilis major cold-shock protein, *Nature*, 364 (1993), 164-168.
- [19] U. Mueller, D. Perl, F. X. Schmid and U. Heinemann, Thermal stability and atomic-resolution crystal structure of the bacillus caldolyticus cold shock protein, *Journal of Molecular Biology*, 297 (2000), 975-988.
- [20] B. Brooks, R. Bruccoleri, B. Olafson, D. States, S. Swaminathan and M. Karplus, Charmm: A program for macromolecular energy, minimization, and dynamics calculations, *Journal of Computational Chemistry*, 4 (1983), 187-217.
- [21] Sánchez R and S. A, Comparative protein structure modeling. Introduction and practical examples with modeller, *Methods in Molecular Biology*, 143 (2000), 97-129.
- [22] S. Spinelli, Q. Z. Liu, P. M. Alzari, P. H. Hirel and R. J. Poljak, The three-dimensional structure of the aspartyl protease from the hiv-1 isolate bru, *Biochimie*, 73 (1991), 1391-1396.
- [23] R. Lapatto, T. Blundell, A. Hemmings, J. Overington, A. Wilderspin, S. Wood, J. R. Merson, P. J. Whittle, D. E. Danley, K. F. Geoghegan, S. J. Hawrylik, S. E. Lee, K. G. Scheld and P. M. Hobart, X-ray analysis of hiv-1 proteinase at 2.7 [angst] resolution confirms structural homology among retroviral enzymes, *Nature*, 342 (1989), 299-302.
- [24] W. Wang and P. A. Kollman, Free energy calculations on dimer stability of the hiv protease using molecular dynamics and a continuum solvent model, *Journal of Molecular Biology*, 303 (2000), 567-582.
- [25] A. P. Wiley, S. L. Williams and J. W. Essex, Conformational motions of hiv-1 protease identi-

- fied using reversible digitally filtered molecular dynamics, *Journal of Chemical Theory and Computation*, 5 (2009), 1117-1128.
- [26] R. Smith, I. M. Brereton, R. Y. Chai and S. B. H. Kent, Ionization states of the catalytic residues in hiv-1 protease, *Nature Structural & Molecular Biology*, 3 (1996), 946-950.
- [27] B. N. Dominy, D. Perl, F. X. Schmid and C. L. Brooks, The effects of ionic strength on protein stability: The cold shock protein family, *Journal of Molecular Biology*, 319 (2002), 541-554.
- [28] M. J. Todd, N. Semo and E. Freire, The structural stability of the hiv-1 protease, *Journal of Molecular Biology*, 283 (1998), 475-488.
- [29] Y. Levy, A. Caflisch, J. N. Onuchic and P. G. Wolynes, The folding and dimerization of hiv-1 protease: Evidence for a stable monomer from simulations, *Journal of Molecular Biology*, 340 (2004), 67-79.
- [30] A. Yang and B. Honig, Structural origins of ph and ionic strength effects on protein stability: Acid denaturation of sperm whale apomyoglobin, *Journal of Molecular Biology*, 237 (1994), 602-614.
- [31] C. N. Schutz and A. Warshel, What are the dielectric "Constants" Of proteins and how to validate electrostatic models?, *Proteins: Structure, Function, and Genetics*, 44 (2001), 400-417.
- [32] A. H. Elcock, Realistic modeling of the denatured states of proteins allows accurate calculations of the ph-dependence of protein stability, *Journal of Molecular Biology*, 294 (1999), 1051-1062.
- [33] J. Antosiewicz, J. A. McCammon and M. K. Gilson, Prediction of ph-dependent properties of proteins, *Journal of Molecular Biology*, 238 (1994), 415-436.
- [34] H.-X. Zhou, Interactions of macromolecules with salt ions: An electrostatic theory for the hofmeister effect, *Proteins: Structure, Function, and Bioinformatics*, 61 (2005), 69-78.
- [35] H.-X. Zhou and F. Dong, Electrostatic contributions to the stability of a thermophilic cold shock protein, *Biophysical Journal*, 84 (2003), 2216-2222.
- [36] K. Ariyama, A theory of surface tension of debye-hückel electrolyte, *Bulletin of the Chemical Society of Japan*, 12 (1937), 32-37.
- [37] L. Onsager and N. Samaras, The surface tension of debye-huückel electrolyte, *The Journal of Chemical Physics*, 2 (1934), 528-536.
- [38] J. Belton, The theory of surface tension of electrolytes, *Transactions of the Faraday Society*, 33 (1937), 1449-1454.
- [39] A. A. Rashin and M. A. Bukatin, Continuum based calculations of hydration entropies and the hydrophobic effect, *The Journal of Physical Chemistry*, 95 (1991), 2942-2944.
- [40] K. Sharp, A. Nicholls, R. Fine and B. Honig, Reconciling the magnitude of the microscopic and macroscopic hydrophobic effects, *Science*, 252 (1991), 106-109.
- [41] K. A. Sharp, A. Nicholls, R. Friedman and B. Honig, Extracting hydrophobic free energies from experimental data: Relationship to protein folding and theoretical models, *Biochemistry*, 30 (1991), 9686-9697.
- [42] A. Ben-Naim, Solvation thermodynamics of nonionic solutes, *The Journal of Chemical Physics*, 81 (1984), 2016-2027.
- [43] T. Simonson and A. T. Bruenger, Solvation free energies estimated from macroscopic continuum theory: An accuracy assessment, *The Journal of Physical Chemistry*, 98 (1994), 4683-4694.
- [44] P. Leroy, A. Lassin, M. Azaroual and L. André, Predicting the surface tension of aqueous 1:1 electrolyte solutions at high salinity, *Geochimica et Cosmochimica Acta*, 74 (2010), 5427-5442.

- [45] T. Arakawa and S. N. Timasheff, Preferential interactions of proteins with salts in concentrated solutions, *Biochemistry*, 21 (1982), 6545-6552.
- [46] D. Perl, U. Mueller, U. Heinemann and F. X. Schmid, Two exposed amino acid residues confer thermostability on a cold shock protein, *Nature Structural Biology*, 7 (2000), 380-383.
- [47] L. Polgar, Z. Szeltner and I. Boros, Substrate-dependent mechanisms in the catalysis of human immunodeficiency virus protease, *Biochemistry*, 33 (1994), 9351-9357.
- [48] L. K. Nicholson, T. Yamazaki, D. A. Torchia, S. Grzesiek, A. Bax, S. J. Stahl, J. D. Kaufman, P. T. Wingfield, P. Y. S. Lam, P. K. Jadhav, C. N. Hodge, P. J. Dommaille and C.-H. Chang, Flexibility and function in hiv-1 protease, *Nature Structural & Molecular Biology*, 2 (1995), 274-280.
- [49] W. R. P. Scott and C. A. Schiffer, Curling of flap tips in hiv-1 protease as a mechanism for substrate entry and tolerance of drug resistance, *Structure (London, England: 1993)*, 8 (2000), 1259-1265.
- [50] A. L. Perryman, J.-H. Lin and J. A. McCammon, Hiv-1 protease molecular dynamics of a wild-type and of the v82f/i84v mutant: Possible contributions to drug resistance and a potential new target site for drugs, *Protein Science*, 13 (2004), 1108-1123.